recycling

Article

Recycling of Pretreated Polyolefin-Based Ocean-Bound Plastic Waste by Incorporating Clay and Rubber

Shawn Martey [1], Keith Hendren [2], Nicholas Farfaras [1], Jesse C. Kelly [2], Matthew Newsome [2], Izabela Ciesielska-Wrobel [3], Margaret J. Sobkowicz [1] and Wan-Ting Chen [1,*]

[1] Department of Plastics Engineering, University of Massachusetts Lowell, Lowell, MA 01854, USA; shawn_martey@student.uml.edu (S.M.); nicholas_farfaras@student.uml.edu (N.F.); margaret_sobkowiczkline@uml.edu (M.J.S.)

[2] Luna Innovations Incorporated, Roanoke, VA 24011, USA; hendrenk@lunainc.com (K.H.); kellyj@lunainc.com (J.C.K.); newsomem@lunainc.com (M.N.)

[3] Department of Textiles, Fashion Merchandising and Design, University of Rhode Island, Kingston, RI 02881, USA; iciewrobel@uri.edu

[*] Correspondence: gracewanting_chen@uml.edu; Tel.: +1-978-934-5371

Abstract: Plastic waste found in oceans has become a major concern because of its impact on marine organisms and human health. There is significant global interest in recycling these materials, but their reclamation, sorting, cleaning, and reprocessing, along with the degradation that occurs in the natural environment, all make it difficult to achieve high quality recycled resins from ocean plastic waste. To mitigate these limitations, various additives including clay and rubber were explored. In this study, we compounded different types of ocean-bound (o-HDPE and o-PP) and virgin polymers (v-LDPE and v-PS) with various additives including a functionalized clay, styrene-multi-block-copolymer (SMB), and ethylene-propylene-based rubber (EPR). Physical observation showed that all blends containing PS were brittle due to the weak interfaces between the polyolefin regions and the PS domains within the polymer blend matrix. Blends containing clay showed rough surfaces and brittleness because of the non-uniform distribution of clay particles in the polymer matrix. To evaluate the properties and compatibility of the blends, characterizations using differential scanning calorimetry (DSC), scanning electron microscopy (SEM), and small-amplitude oscillatory shear (SAOS) rheology were carried out. The polymer blend (v-LDPE, o-HDPE, o-PP) containing EPR showed improved elasticity. Incorporating additives such as rubber could improve the mechanical properties of polymer blends for recycling purposes.

Keywords: plastic waste; polymer blends; compatibilization; recycling; rubber; clay

1. Introduction

Most plastic waste streams contain a mixture of different polymers. For example, an estimated amount of 182,085 metric tons of plastics is discarded into Brazil's Amazon river and enters the Atlantic ocean [1,2]. These plastics are ingested by living things including fish, turtles, etc. [1,3,4]. In particular, polyolefins including high-density polyethylene (HDPE), low-density polyethylene (LDPE), and polypropylene (PP) account for 82% of the ingested plastics [5].

Sorting different polymers to a high degree of purity is technically challenging and adds a costly step for recycling. Blending of polymers is thus considered as a cost-effective method to recycle comingled plastic waste [6]. However, polymers do not blend well. The small entropic gain during mixing makes most polymers immiscible [7]. In melt blending, mechanical, thermal, optical, chemical, or rheological properties of recycled polymers could be weakened due to immiscibility of polymers. These inferior properties result from the poor interaction between the phases of the constituent polymers in the blend. Improvement of adhesion between the polymer phases can help attain satisfactory performance of the blend [8,9].

To improve compatibility of immiscible blends, additives are commonly used. One of the most used additives is compatibilizers [10]. Compatibilizers are added to enhance the interaction between polymer phases. Compatibilizers such as block or graft copolymers serve as surfactants or covalent linkages at the interface, lowering interfacial tension and improving adhesion between phases [11]. Compatibilization is mostly achieved by reactive means. This strategy includes trans-reactions, reactive formation of copolymers, formation of ionically bonded structures, and the breaking and recombination of chains via mechano-chemical blending [12–14]. In reactive processing, bonds are formed between dissimilar polymers during blending, and this helps in compatibilizing the immiscible phases of the blend and provides a stable morphology. Improper compatibilization of blends may lead to early mechanical failure due to weakness at the interfaces between phases [15,16].

Studies have been conducted to improve polymer properties by blending. Rivas et al., (2001) studied the possible increase in tensile strength and heat deflection temperature (HDT) of ABS in PET/ABS blend. It was reported that a blend with up to 10 wt% waste PET in ABS showed a higher tensile strength and higher heat deflection temperature when compared to virgin ABS [17]. This is just one example of how polymer properties have been improved by blending.

Another method to improve the mechanical/thermal properties of recycled plastics is the addition of additives such as fillers, which could be natural (e.g., biomass), inorganic (e.g., clay), or elastomers (e.g., rubber) [10]. Additives have been used as processing aids (to improve polymer processability), antioxidants (to delay degradative processes), fillers (to decrease cost and enhance performance), impact modifiers (to increase impact strength), and compatibilizers (to improve blend morphology and interfacial adhesion) [18].

Clays have been used to improve many different aspects of the performance of polymers. These clays are added to the polymer matrix of thermoplastics to improve their flame retardancy [19,20], barrier properties [19,21], mechanical properties [19], thermal expansion coefficients [22], and gas barrier properties [23]. These property improvements depend on the structural configuration and interfacial interaction between the polymer and the clay [24]. Some studies have shown that to include exfoliated clay in polymer blends can compatibilize the phases [25,26]. Particle shape (spheres, rods), particle radius relative to the radius of gyration of polymer, surface chemistry, and processing method are a few factors that influence the dispersion of clay into nano-size particles and the final properties (e.g., mechanical and thermal properties) of the blends [27]. Exfoliation of clay is desired in polymer blends, since properly exfoliated clay can migrate to the blend interface, enhancing the compatibility between the two phases by altering the viscosity of the matrix and preventing droplet coalescence during mixing [28–30]. If exfoliation is not achieved, the micron-scale clay particles will instead serve as filler particles that can reinforce the blend, but without enhancement of phase compatibility [31]. Blending of rubbers such as ethylene-propylene-diene monomer (EPDM) with polymers is an alternative method for improving properties of the blend. An EPDM/PP blend using maleated PP as a compatibilizer with surface-oxidized rubber has shown an improvement in mechanical properties of the blend [32].

Waste polymers tend to have inferior properties due to degradation; thus, the inclusion of virgin polymers in the blend has the tendency to improve the lower properties of the waste polymers. From an economic and environmental point of view, inclusion of virgin polymers in waste blend may improve the quality of the blend and also reduce the waste disposal problem [6]. Therefore, blending virgin and waste polymers could be a good strategy to handle waste polymers.

A large number of blending/compatibility studies have been made using virgin polymers and incorporating compatibilizers. To the best of our knowledge, similar studies have not been conducted using plastic waste recovered from the marine environment (e.g., ocean-bound plastic waste), which could be harmful not only to the marine ecosystem but also to human beings [33–35]. In addition, ocean-bound plastic waste usually has inferior properties (as compared to virgin plastics) due to environmental degradation. In

light of this, this paper aims to evaluate the effects of rubber and clay on the performance of polymer blends composed of polyolefin-based ocean-bound plastic waste (which is primarily made of HDPE and PP) [36] In addition, HDPE and PP based ocean-bound plastic waste (o-HDPE and o-PP) were also blended with another two commodity plastics (virgin LDPE, v-LDPE and virgin PS, v-PS) to understand the polymer blend systems composed of polyolefins (o-HDPE, o-PP and v-LDPE) and polyolefins/PS mixture.

Melt mixing was carried out using a micro-compounder. The thermal, mechanical, and rheological properties of the blends were compared to individual waste plastics for recycling purposes. The compatibilizer efficacy using clay, rubber, and compatibilizer was also evaluated. The results obtained from this study are expected to help optimize blend composition and recycling ocean-bound plastic waste.

2. Results and Discussion

2.1. General Observations of Polymer Blends

As Table 1 shows, polymer blends were created with virgin LDPE (v-LDPE) and PS (v-PS), ocean-bound HDPE (o-HDPE) and PP (o-PP), as well as additives (clay, SMB, and EPR). The compounded filaments were visually evaluated first. Figure S1 (Supplementary Materials) shows images of blended filaments. In general, all blends containing v-PS showed a rough surface and were brittle (Table 1). Owing to great structural differences and the minimal entropic gain from mixing polymers, PS did not blend well with the polyethylene and polypropylene components [37]. Blends containing clay typically remained as aggregates in the filament. Filaments containing 30% of clay were very brittle and had clay particles visible on the surface, while the filament with 10% clay was flexible but still showed visible clay particles. The filament with 25% EPR was very flexible due to the elastic properties of EPR. A similar characteristic was observed by Bertin et al. when EPR was used as compatibilizer in the study of virgin and recycled LDPE/PP blends [38].

Table 1. Polymer blends prepared by using virgin LDPE (v-LDPE) and PS (v-PS), ocean-bound HDPE (o-HDPE) and PP (o-PP), as well as additives (clay, SMB, and EPR).

	Base Polymers				Additives			Characteristics of Polymer Blends
	v-LDPE	o-HDPE	o-PP	v-PS	Clay	SMB	EPR	
1	23 g	23 g	23 g	-	30 g	-	-	Brittle, Poor dispersion of clay in the blend
2	30 g	30 g	30 g	-	10 g	-	-	Flexible; Poor dispersion of clay
3	33 g	33 g	33 g	-	-	-	-	Flexible
4	25 g	25 g	25 g	-	-	-	25 g	Very flexible
5	19 g	19 g	19 g	19 g	-	5 g	19 g	Flexible
6	25 g	25 g	25 g	25 g	-	-	-	Quite brittle
7	23 g	23 g	23 g	23 g	8 g	-	-	Flexible, Poor dispersion of clay in the blend with visible clay particles
8	17 g	17 g	17 g	17 g	10 g	5 g	17 g	Flexible

2.2. Differential Scanning Calorimetry (DSC)

DSC was used to identify any increased compatibility behavior of the blends. Table 2 and Figure 1 show the DSC data obtained from the second heating cycle of polymer blends from −50 °C to 300 °C. The thermogram shows two endothermic peaks of the crystalline portions of the constituent polymers of the blends. Ocean PP (o-PP) shows two endothermic peaks at 130 °C and 162 °C. This may be due to the presence of PE contamination in the recycled PP [39]. Another possibility could be that the PP is actually a copolymer with some ethylene to enhance the impact strength [40] PE showed a larger enthalpy of fusion due to a higher composition of both HDPE and LDPE in all the blends. For the blends, only two distinct peaks were observed although the blends contained three polymers. This is attributed to the nearly identical melting temperatures of the PE grades; thus, the two materials could not be resolved separately [41]. However, a slight shoulder is observed around 120 °C which is likely from the o-LDPE phase. It is not clear from DSC analysis

whether perfect miscibility occurred between HDPE and LDPE. A similar phenomenon is seen in other studies, and it was speculated that some miscibility is possible between the LDPE and HDPE. Although branching extent was not known in this study, other works show that lower branching contents of LDPE improve miscibility of HDPE and LDPE [42–45].

Table 2. Thermal transition properties (including melting temperature, enthalpy of melting and crystallinity) of polymer blends composed of o-HDPE, v-LDPE and o-PP (from the second heating curve of DSC).

Polymers	o-HDPE			v-LDPE			o-PP		
	T_m (°C)	ΔH (J/g)	%X	T_m (°C)	ΔH (J/g)	%X	T_m (°C)	ΔH (J/g)	%X
v-LDPE	-	-	-	112.7	137.3	46.9	-	-	-
o-HDPE	133.1	201.6	68.8	-	-	-			
o-PP	130.4	41.8	20.2	-	-	-	162.2	50.9	24.6
o-HDPE (33%) _v-LDPE (33%) _o-PP (33%)	129.7	197.6	67.4	-	-	-	162.0	54.6	26.4
o-HDPE (25%) _v-LDPE (25%) _o-PP (25%) _EPR (25%)	129.8 *	212.9 *	72.7 *	-	-	-	164.5	57.5	27.8
o-HDPE (30%) _v-LDPE (30%) _o-PP (30%) _clay (10%)	129.9	173.0	59.1	-	-	-	162.9	37.8	18.2

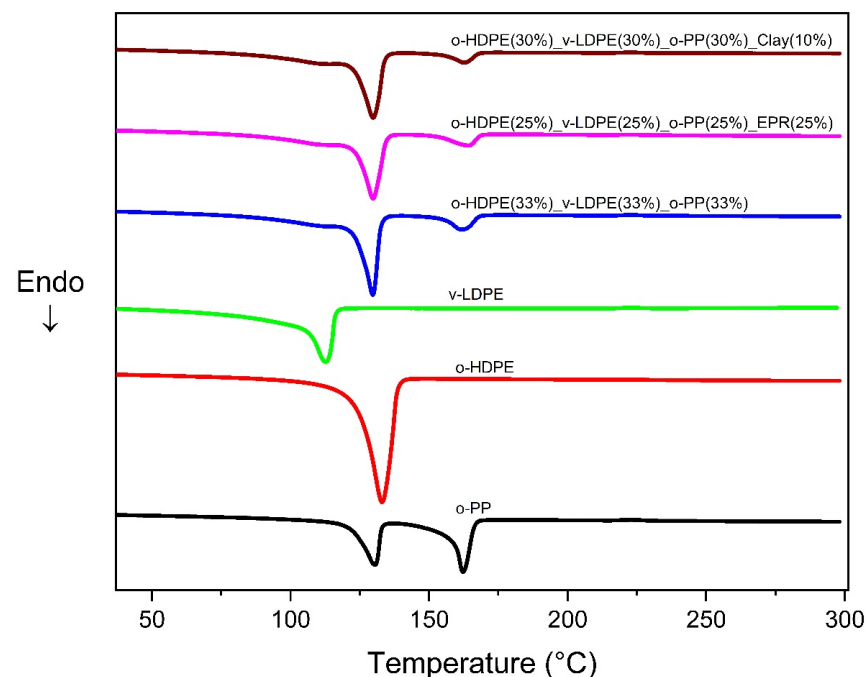* o-HDPE and v-LDPE appeared as one peak in DSC.

Figure 1. Differential scanning calorimetry of polymer blends composed of o-HDPE, v-LDPE, o-PP, EPR and clay.

2.3. Scanning Electron Microscopy (SEM)

To evaluate the effects of clay and EPR on the morphology of the ternary blends, three ternary polymer blends (o-HDPE (30%)_o-PP (30%)_v-LDPE (30%), o-HDPE (30%)_o-PP (30%)_v-LDPE 30%)_clay (10%), and o-HDPE (25%)_o-PP (25%)_v-LDPE (25%)_EPR (25%)) were observed under SEM. The study of the morphological characteristics of the selected blends was essential to determine the phase interactions and miscibility of the constituent polymers. The fractured surface was investigated for the blends (Figure 2). The results indicate that the blend without any additive showed large voids, and this could be associated with the incompatibility of the phases. However, results from blends containing

clay and EPR showed smaller voids with the exception of a large chunk of EPR appearing. This large chunk may be as a result of poor shearing of the EPR during micro-compounding at low speed. In addition, the EPR used was not received in the form of pellets, but the particle size was manually reduced before compounding. This result also indicates that the particle size of EPR is an important factor to consider when including EPR in a blend. Apart from the large chunks observed in the blend with EPR, there was generally a reduction of the void size in the blend. Increasing the speed of the micro-compounder may reduce the particle size of the EPR due to an increase in shear stress.
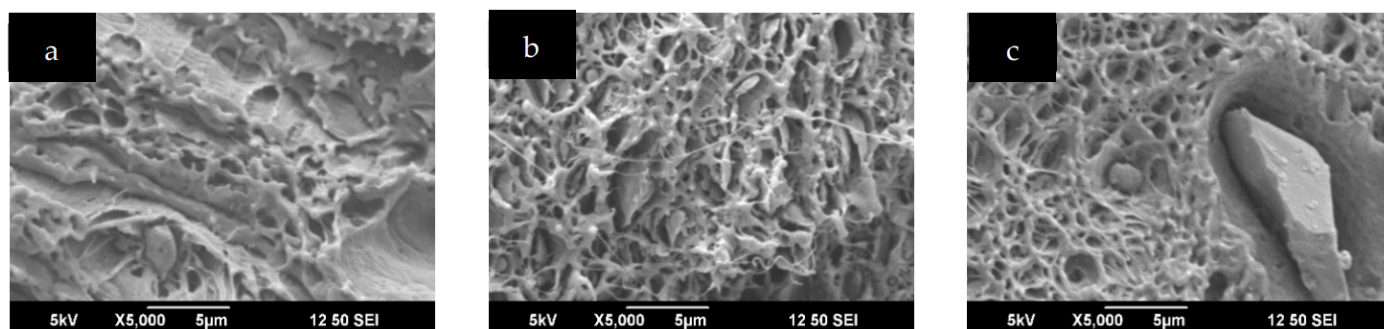

Figure 2. SEM images of selected ternary blends: (**a**) o-HDPE (30%) _o-PP (30%)_v-LDPE (30%), (**b**) o-HDPE (30%)_o-PP (30%)_v-LDPE 30%)_clay (10%), (**c**) o-HDPE (25%)_o-PP (25%)_v-LDPE (25%)_EPR (25%).

Theories show the possibility of determining the interfacial energy at the boundary of two polymers [46,47]. The miscibility of polymers is associated with the changes in the free surface energy of the polymer blends. This can be studied using surface-sensitive techniques such as contact angle goniometry, atomic force microscopy and X-ray photo-electron spectroscopy [48,49]. This could be studied in future research work to advance the fundamental understanding of the polymer blend system. For example, the miscibility of styrene-acrylonitrile/ethylene-propylene-diene blend was estimated through changes of the surface free energy between the interfaces by Sirocic et al. [50]. The surface energy also shed some light regarding the governing mechanism of fiber-matrix adhesion in a polypropylene/polyamide carbon fiber reinforced blend [51]. Although beyond the scope of this study, we predict that the interfacial energy between polyolefins could be lowered by clay that is properly exfoliated and segregated to the interfaces.

2.4. Rheology

A strain sweep was run to determine a strain amplitude in the linear viscoelastic regime for the frequency sweep. A 10% strain was selected and used for further testing (Figure S2). Figure 3a shows the plot of complex viscosity versus angular frequency. The individual o-PP and o-HDPE both show a Newtonian plateau at low frequency, whereas the v-LDPE is more shear thinning in character over the whole frequency range. There is an increase in viscosity at low frequencies in all the blends, reflecting the influence of the v-LDPE in the blends. As Figure 3a shows, no plateau was observed for all the polymer blends tested and thus no Newtonian behavior was found for all the blends. Overall, o- PP and v-LDPE had the lowest magnitude of the viscosity. However, the viscosities of the o- PP and v-LDPE polymer blend increased when they were blended with o-HDPE, EPR, and clay. The clay and EPR may have acted like solid fillers, immobilizing chains at the interfaces and increasing the viscosities of the blend.

Figure 3b shows the storage modulus of the blends versus the angular frequency. Storage modulus describes the elasticity of the polymers. At lower frequency, the blends with LDPE show slight terminal plateauing behavior associated with a high degree of molecular entanglement [52]. In the high angular frequency regime, not much difference

is seen in the storage modulus of the blends. This suggests that segmental motions of the polymer backbones were unaffected by the clay and EPR.
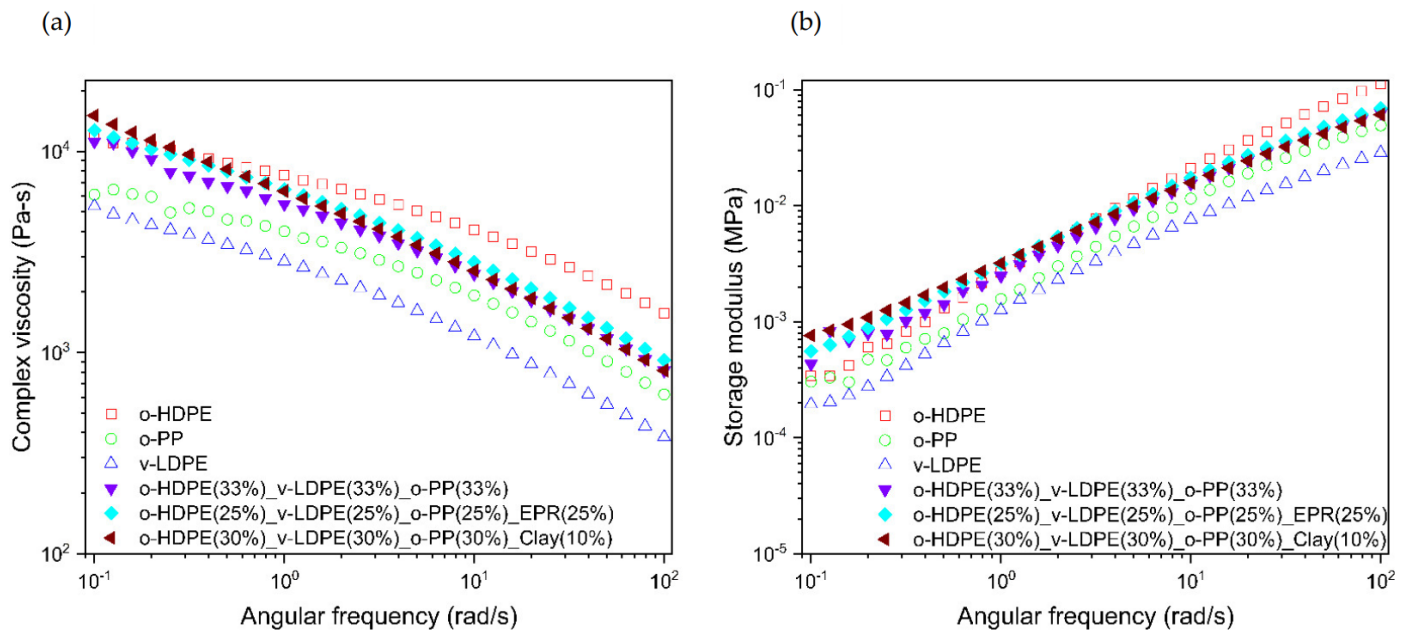
(a)   (b)

Figure 3. (**a**) Complex viscosity versus angular frequency (**b**) Storage modulus versus angular frequency.

2.5. Tensile Testing

Single virgin and ocean plastic resins (unmixed) were compression molded to understand their processibility and mechanical properties using a traditional molding technique. Compression molded virgin plastics (unmixed) showed a slightly higher flexibility and strength compared to their OPW counterparts. These same single resins (virgin and OPW) were also processed into filaments using a 3-Devo 350 Composer and 3D printed on the Creality 3-D printer. Tensile properties of the 3D printed specimens (unmixed) were similar to those of virgin plastics; however, there were noticeable improvement in the modulus and overall toughness of the 3D printed OPWs compared to their 3D printed virgin plastic counterparts and, in some cases, the compression molded virgin plastic material. When blending both virgin, OPW, and virgin/OPW materials (various types of resin), the 3D printed tensile specimens consistently outperformed the compression molded parts in terms of toughness, indicating that unique properties can be provided by 3D printing of these thermoplastics. In compression molded plastics blends, there was significant phase separation. This effect was likely due to slow cooling and a longer time scale for the resins to phase separate due to immiscibility between the polymers. The extruded and 3D printed plastic blends showed reduced phase separation and improved properties relative to their compression molded counterparts due to rapid cooling on the 3D printer bed, which shortened the time scale for phase separation to occur. These drastically different time scales allowed for improved miscibility of blends and their mechanical properties and were the primary motivation for utilizing 3D printing in this paper. However, it is acknowledged that one may find applications for the compression molded parts that could still bring significant value, such as fencing posts, playground surfacing, and other low flexibility applications. Additional research to compare different processing methods using this formulation of material is therefore recommended. For 3D printed filaments, based on the flexibility and ease of processing, these materials could be used for making toys, tents, mats, and other recreational applications. Table 3 and Figure 4 shows the mechanical properties of the individual polymers and the blends. The addition of clay improved the toughness of polymer blend (as shown in Figure 4), and the addition of EPR largely did the same. EPR improved the elongation of the blend due to its elastic nature, but the ultimate tensile strength of the blend decreased. Notably, the addition of clays led to 3-D printer

nozzle clogging, and the addition of EPR led to softening of the polymer to such an extent that the feedgear of the printer cut the polymer stripping material and disabled feeding. Interestingly, the o-HDPE and v-LDPE were the only polymers that were able to undergo strain hardening as printed polymers.

Table 3. Mechanical properties (including ultimate tensile strength and elongation at peak load) of polymer blends composed of o-HDPE, v-LDPE, and o-PP (from the printing tensile bars, n = 3).

Polymers	Ultimate Tensile Strength (MPa)	Elongation at Peak Load (%)
v-LDPE	13.3 ± 0.6	324.6 ± 66.1
o-HDPE	22.3 ± 0.8	25.3 ± 1.1
o-PP	31.6 ± 2.0	19.1 ± 4.4
v-LDPE (33.3%)_o-HDPE (33.3%)_o-PP (33.3%)	21.4 ± 0.9	21.7 ± 1.4
v-LDPE (30%)_o-PP (30%)_o-HDPE (30%)_clay (10%) *	16.4	24.2
v-LDPE (25%)_o-PP (25%)_o-HDPE (25%)_EPR (25%) *	11.2	540.5

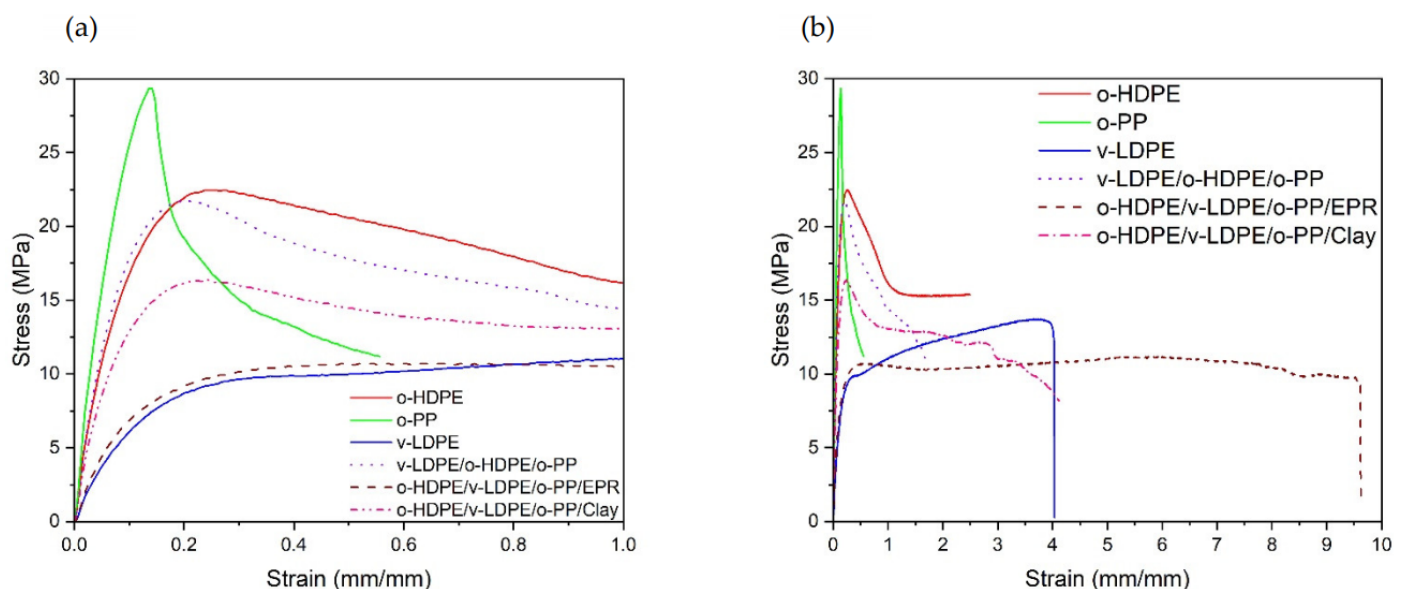* The sample clogged the nozzle so only one sample was printed for these two samples.

Figure 4. Mechanical properties of polymer blends made of ocean-bound plastic waste with a strain of (**a**) 0–1 mm/mm and (**b**) 0–10 mm/mm.

3. Materials and Methods

Table 4 summarizes the properties of polymers used in this study. The polymer types used in this work were virgin high-density polyethylene (v-HDPE) from ExxonMobil (BA50-100), virgin low-density polyethylene (v-LDPE) from ExxonMobil (LD123.LN), virgin polystyrene (v-PS) from Certene (SGM-140), ocean-bound high-density polyethylene (o-HDPE) (OR.190222), and ocean-bound polypropylene (o-PP) (OR.190252) samples were graciously provided by Oceanworks. Additives used in this study included a styrene-multi-block-copolymer (SMB), a functionalized clay developed by Luna Innovations, and ethylene-propylene-based copolymer rubber (EPR) from ExxonMoobil (Vistalon™ 404) with ethylene content of 44.5 wt% and a low Mooney viscosity of 28 MU [53]. The EPR received was not in pellet form (i.e., was in irregular shapes of chunks) and the size of EPR was manually reduced by chopping it into smaller pieces.

Table 4. Properties of polymers used in this study.

	ExxonMobil (BA50-100) [a]	ExxonMobil (LD123.LN)	Certene [TM] SGM-140	Oceanworks (OR.190222)	Oceanworks (OR.190252)
Density (g/cm^3)	0.949	0.923	1.05	0.94–0.96	0.91–0.93
Melt Index (g/10 min)	<0.10 (190 °C/2.16 kg)	2.4 (190 °C/2.16 kg)	14 (200 °C/5 kg)	0.75 (190 °C/2.16 kg)	3.55 (190 °C/2.16 kg)
Vicat softening Temperature (°C)	120.0	92.0	92.8	N/A	N/A

[a] [Ref number] [54–58].

3.1. Compounding of Materials

Recycled blends were prepared by mixing virgin LDPE, virgin PS, recycled ocean HDPE, recycled ocean PP, EPR SMB, and clay in various ratios. The blends were formulated with nearly equal fractions of each included polymer and a minimal proportion of additives. Blends with virgin polymer are labeled with V (e.g., v-LDPE) while those with recycled ocean plastic are labeled with O (e.g., o-HDPE). Compounding was done in a conical twin screw micro compounder (Xplore[TM] HT-15, Sittard, The Netherlands) at a screw speed of 15 rpm and a temperature of 200–240 °C [53]. Samples were extruded as filaments with a diameter of about 0.5 cm.

3.2. Extruding Printer Filament

A 3-Devo 350 Composer (3devo, Claymont, DE, United States) is a filament making machine with automatic spooling. It requires roughly 150–200 g of material. For virgin or recycled pure filament (e.g., 100% o-HDPE, 100% v-LDPE) pellets were added to the hopper directly. Filaments of compounded materials from the DSM Xplore[TM] were pelletized using tin snips and put into the 3-Devo hopper. Materials were purged between runs with v-HDPE. Contamination was prevented by extruding filament until the color of the filament became consistent and this filament was used for 3-D printing. Between different samples and prior to purging the 3Devo, the contents of the hopper were removed from the feed screw with a vacuum. It requires roughly 150–200 g of material. In using the 3-Devo Composer the material was put into the hopper and the material, when the color became consistent, was used for printing applications. Before adding new materials to the 3Devo the contents of the hopper were removed from the feed screw with a vacuum. In using this machine, the processing conditions for the highest melting point component were used. The processing temperatures for the polymers were set by first setting the feed and nozzle temperature to about 30% above the melting temperature of that class of polymer. The other two temperatures, the mixing temperatures, were set to 10–20 °C greater than the nozzle and feed temperatures. If necessary, to obtain a more consistent filament diameter the nozzle and mixing temperatures were altered.

3.3. Printing Tensile Speciments (i.e., Dogbones)

A Creality 3-D printer (nozzle diameter of 0.4 mm) with the Cura software (Ultimaker, Utrecht, the Netherlands) was used to print dogbone specimens. For most samples, the printer was set to 270 °C and the bed temperature was set to 60 °C. The printer was able to extrude all specimens at this temperature. These conditions were chosen to observe how these polymers would behave at temperatures intended for higher processing temperature polymers such as PET. The low bed temperature allows these polymers to be compared to print conditions for acrylonitrile-butadiene-styrene (ABS) print filament. The samples were printed with 100% infill with a crosshatch pattern on the dogbones and a linear pattern through the gauge area of the dogbones. ASTM D638 coupons were printed in all cases. The thickness of the printed dogbones ranged between 0.05–0.13 inches and the width ranged between 0.129–0.165 inches. Compression molded samples had a thickness of 0.54–0.59 inches and a width of 0.16 inches.

3.4. Characterization of Polymer Blends

3.4.1. Differential Scanning Calorimetry

The melting and crystallization behavior of the polymer blends were determined using differential scanning calorimeter (Discovery RES-02-002-B, TA Instruments, New Castle, DE, USA). Aluminum hermetic pans were used for both reference and blended samples. A heat/cool/heat cycle was used for this experiment. Samples (3–6 mg) were heated at a rate of 10 °C/min to 300 °C and cooled at 10 °C/min to −50 °C. The same heating procedure was repeated. The percent crystallinity of the blended samples was determined using the second heating curve. The percent crystallinity was estimated as the ratio of the enthalpy of the heat of fusion of the sample, ΔH_f, to the mass fraction f of the heat of fusion of 100% crystalline of the polymer, ΔH_{fo}, (Equation (1)).

$$X_C\% = \frac{\Delta H_f}{f \times \Delta H_{fo}} \times 100\% \tag{1}$$

3.4.2. Scanning Electron Microscopy

The phase interactions between individual polymers in the blends were investigated using a scanning electron microscope (SEM, JEOL JSM 6390, Tokyo, Japan). Filaments were immersed in liquid nitrogen for 10 min and fractured after they became brittle. Fractured samples were coated with gold for 120 s using a vacuum sputter coater (Denton vacuum desk IV, Denton Vacuum, LLC, Moorestown, NJ, USA). The morphology of the blend was observed under the microscope at a beam energy of 5 kV.

3.4.3. Rheology

The rheological behavior of the blends in the second stage was determined using an ARES-G2 rotational rheometer (ARES 401001.901, TA instrument, New Castle, DE, USA). Sample disks of 25 mm diameter were molded using a micro injection molding machine (Xplore Instruments BV, Sittard, The Netherlands) at 190 °C. A strain sweep was performed at 200 °C to select a strain percentage in the linear viscoelastic region (LVR) for the frequency sweep. A frequency sweep was also performed at 200 °C and at a strain amplitude of 10% (determined to be in the LVR from the strain sweep) over an angular frequency of 100 rad/s to 0.1 rad/s with a constant plate gap of 1.5 mm [59] Click or tap here to enter text.

3.4.4. Tensile Testing

Single virgin and ocean plastic resins (unmixed) were compression molded to understand their processibility and mechanical properties using a traditional molding technique. Tensile testing was conducted on an ADMET tensile tester equipped with serrated clamps at a crosshead sped of 2 in·min^{-1}. The tensile specimens were ASTM D638 Type V dogbones, and the thickness of each sample was measured prior to testing. The tensile data was taken without an extensometer, and the outputs from the tensile testing were elongated at break and peak yield strength. The only samples that had a greater ultimate tensile stress than yield stress were the v-HDPE and v-LDPE samples.

4. Conclusions

Polymer blending could be an effective and environmentally conscious means for recycling of plastics materials. Blending of polymers can improve the properties of individual polymers. The incorporation of additives such as compatibilizers, clay, and rubber also has an influence on the properties of the polymer materials. There was no evidence of improvement of miscibility from the differential scanning calorimetry results since the glass transition temperatures of the individual polymers could not be resolved in the blends. Scanning electron microscopy confirmed the immiscibility of the blends without any additive. However, aggregated particles were seen in the blend containing clay. Based on previous literature findings, clay could well have improved the compatibility of the blends

if exfoliated properly. The exfoliation of the clay could be improved by increasing the intensity of mixing; this would help to reduce the particle size to improve the compatibility. EPR improved the elasticity of the blend. Incorporation of additives such as clay and rubber in appropriate quantities, with quality mixing and proper exfoliation of the clay into waste polymers blends, could improve properties of blends and render the polymers reusable.

Supplementary Materials: The following are available online at https://www.mdpi.com/article/10.3390/recycling7020025/s1, Figure S1: The blended samples composed of: (a) o-HDPE (23 g) _o-PP (23 g)_v-LDPE(23 g)_clay (30 g); (b) o-HDPE (30 g) _o-PP (30 g)_v-LDPE(30 g)_clay (10%); (c) o-HDPE (33 g) _o-PP (33 g)_v-LDPE(33 g); (d) o-HDPE (25 g) _o-PP(25 g)_v-LDPE(25 g)_EPR(25 g), (e) o-HDPE (19 g) _o-PP (19 g)_v-LDPE(19 g)_v-PS(19 g)_SEBS(5 g)_EPR(19 g), (f) o-HDPE (25 g) _o-PP (25 g)_v-LDPE(25 g)_v-PS(25 g), (g) o-HDPE (23 g) _o-PP (23 g)_v-LDPE(23 g)_v-PS(23 g)_clay(10 g), (h) o-HDPE (17 g) _o-PP (17 g)_v-LDPE(17 g)_v-PS(17 g)_clay(10 g)_SEBS(5 g)_ EPR(17 g); Figure S2: Strain sweep of samples.

Author Contributions: Conceptualization, S.M., K.H, J.C.K., W.-T.C. and I.C.-W.; methodology, S.M., K.H., N.F., J.C.K., M.N. and I.C.-W.; software, S.M. and K.H.; validation, S.M., K.H., M.N. and N.F.; formal analysis, S.M. and K.H.; investigation, S.M., K.H. and M.N.; resources, J.C.K., M.J.S. and W.-T.C.; data curation, S.M. and K.H.; writing—original draft preparation, S.M.; writing—review and editing, S.M., K.H., J.C.K., N.F., M.N., I.C.-W., M.J.S. and W.-T.C.; visualization, S.M. and K.H.; supervision, J.C.K., M.J.S., W.-T.C. and I.C.-W.; project administration, J.C.K., I.C.-W. and W.-T.C.; funding acquisition, J.C.K., I.C.-W. and W.-T.C. All authors have read and agreed to the published version of the manuscript.

Institutional Review Board Statement: Not applicable.

Informed Consent Statement: Not applicable.

Data Availability Statement: The data presented in this study are available upon request from the corresponding author.

Conflicts of Interest: The authors declare no conflict of interest.

References

1. Andrady, A.L. Microplastics in the marine environment. *Mar. Pollut. Bull.* **2011**, *62*, 1596–1605. [CrossRef] [PubMed]
2. Jambeck, J.R.; Geyer, R.; Wilcox, C.; Siegler, T.R.; Perryman, M.; Andrady, A.; Narayan, R.; Law, K.L. Plastic waste inputs from land into the ocean. *Science* **2015**, *347*, 768–771. [CrossRef] [PubMed]
3. Devi, S.S.; Sreedevi, A.V.; Kumar, A.B. First report of microplastic ingestion by the alien fish Pirapitinga (Piaractus brachypomus) in the Ramsar site Vembanad Lake, south India. *Mar. Pollut. Bull.* **2020**, *160*, 111637. [CrossRef]
4. Athey, S.N.; Albotra, S.D.; Gordon, C.A.; Monteleone, B.; Seaton, P.; Andrady, A.L.; Taylor, A.R.; Brander, S.M. Trophic transfer of microplastics in an estuarine food chain and the effects of a sorbed legacy pollutant. *Limnol. Oceanogr. Lett.* **2020**, *5*, 154–162. [CrossRef]

5. Jung, M.R.; Balazs, G.H.; Work, T.M.; Jones, T.T.; Orski, S.V.; Rodriguez, C.V.; Beers, K.L.; Brignac, K.C.; Hyrenbach, K.D.; Jensen, B.A.; et al. Polymer Identification of Plastic Debris Ingested by Pelagic-Phase Sea Turtles in the Central Pacific. *Environ. Sci. Technol.* **2018**, *52*, 11535–11544. [CrossRef] [PubMed]

6. Ragaert, K.; Delva, L.; Van Geem, K. Mechanical and chemical recycling of solid plastic waste. *Waste Manag.* **2017**, *69*, 24–58. [CrossRef] [PubMed]

7. Utracki, L.A.; Wilkie, C.A. *Polymer Blends Handbook*; Springer: Dordrecht, The Netherlands, 2014.

8. Pang, Y.X.; Jia, D.M.; Hu, H.J.; Hourston, D.J.; Song, M. Effects of a compatibilizing agent on the morphology, interface and mechanical behaviour of polypropylene/poly(ethylene terephthalate) blends. *Polymer* **2000**, *41*, 357–365. [CrossRef]

9. Xanthos, M.; Young, M.W.; Biesenberger, J.A. Polypropylene/polyethylene terephthalate blends compatibilized through functionalization. *Polym. Eng. Sci.* **1990**, *30*, 355–365. [CrossRef]

10. Scaffaro, R.; Botta, L.; Mistretta, M.C.; La Mantia, F.P. Processing-morphology-property relationships of polyamide 6/polyethylene blend-clay nanocomposites. *Express Polym. Lett.* **2013**, *7*, 873–884. [CrossRef]

11. Ebadi, H.; Yousefi, A.A.; Ouroumiehei, A.B.D.A. Reactive extrusion and barrier properties of PP/PET films. *Iran. Polym. J.* **2007**, *16*, 10.

12. Calderón, B.A.; Thompson, C.W.; Barinelli, V.L.; McCaughey, M.S.; Sobkowicz, M.J. Effect of exchange reactions and free radical grafting on the high-speed reactive extrusion of poly(butylene succinate) and poly(propylene carbonate) blends. *Polym. Eng. Sci.* **2019**, *59*, 1986–1998. [CrossRef]

13. Gug, J.I.; Sobkowicz, M.J. Improvement of the mechanical behavior of bioplastic poly(lactic acid)/polyamide blends by reactive compatibilization. *J. Appl. Polym. Sci.* **2016**, *133*, 133. [CrossRef]

14. Muthuraj, R.; Misra, M.; Mohanty, A.K. Biodegradable compatibilized polymer blends for packaging applications: A literature review. *J. Appl. Polym. Sci.* **2018**, *135*, 45726. [CrossRef]

15. Shaw, W.J.D. Polymer Alloy Material and Process for Production Thereof. U.S. Patent No. 5,367,048, 22 November 1994.

16. Utracki, L.A. Compatibilization of polymer blends. *Can. J. Chem. Eng.* **2002**, *80*, 1008–1016. [CrossRef]

17. Rivas, B.L.; Pereira, E.D. Blends of acrylonitrile-butadiene-styrene/waste poly(ethylene terephthalate) compatibilized by styrene maleic anhydride. *J. Appl. Polym. Sci.* **2001**, *80*, 2593–2599. [CrossRef]

18. La Mantia, F.P. The Role of Additives in the Recycling of Polymers. *Macromol. Symp.* **1998**, *135*, 157–165. [CrossRef]

19. Huitric, J.; Ville, J.; Médéric, P.; Moan, M.; Aubry, T. Rheological, morphological and structural properties of PE/PA/nanoclay ternary blends: Effect of clay weight fraction. *J. Rheol.* **2009**, *53*, 1101–1119. [CrossRef]

20. Tang, Y.; Hu, Y.; Wang, S.; Gui, Z.; Chen, Z.; Fan, W. Preparation of poly(propylene)/clay layered nanocomposites by melt intercalation from pristine montmorillonite (MMT). *Polym. Adv. Technol.* **2003**, *14*, 733–737. [CrossRef]

21. Ke, Z.; Yongping, B. Improve the gas barrier property of PET film with montmorillonite by in situ interlayer polymerization. *Mater. Lett.* **2005**, *59*, 3348–3351. [CrossRef]

22. Yang, Y.; Zhu, Z.K.; Yin, J.; Wang, X.Y.; Qi, Z.E. Preparation and properties of hybrids of organo-soluble polyimide and montmorillonite with various chemical surface modification methods. *Polymer* **1999**, *40*, 4407–4414. [CrossRef]

23. Messersmith, P.B.; Giannelis, E.P. Synthesis and barrier properties of poly(ε-caprolactone)-layered silicate nanocomposites. *J. Polym. Sci. Part A Polym. Chem.* **1995**, *33*, 1047–1057. [CrossRef]

24. Huang, J.C.; Zhu, Z.K.; Yin, J.; Qian, X.F.; Sun, Y.Y. Poly(etherimide)/montmorillonite nanocomposites prepared by melt intercalation: Morphology, solvent resistance properties and thermal properties. *Polymer* **2001**, *42*, 873–877. [CrossRef]

25. Mofokeng, T.G.; Ray, S.S.; Ojijo, V. Structure–property relationship in PP/LDPE blend composites: The role of nanoclay localization. *J. Appl. Polym. Sci.* **2018**, *135*, 46193. [CrossRef]

26. Vazquez, A.; López, M.; Kortaberria, G.; Martín, L.; Mondragon, I. Modification of montmorillonite with cationic surfactants. Thermal and chemical analysis including CEC determination. *Appl. Clay Sci.* **2008**, *41*, 24–36. [CrossRef]

27. Taguet, A.; Cassagnau, P.; Lopez-Cuesta, J.M. Structuration, selective dispersion and compatibilizing effect of (nano)fillers in polymer blends. *Prog. Polym. Sci.* **2014**, *39*, 1526–1563. [CrossRef]

28. Gelfer, M.Y.; Song, H.H.; Liu, L.; Hsiao, B.S.; Chu, B.; Rafailovich, M.; Si, M.; Zaitsev, V. Effects of organoclays on morphology and thermal and rheological properties of polystyrene and poly(methyl methacrylate) blends. *J. Polym. Sci. Part B Polym. Phys.* **2002**, *41*, 44–54. [CrossRef]

29. Si, M.; Araki, T.; Ader, H.; Kilcoyne, A.L.D.; Fisher, R.; Sokolov, J.C.; Rafailovich, M.H. Compatibilizing bulk polymer blends by using organoclays. *Macromolecules* **2006**, *39*, 4793–4801. [CrossRef]

30. Moghbelli, E.; Sue, H.J.; Jain, S. Stabilization and control of phase morphology of PA/SAN blends via incorporation of exfoliated clay. *Polymer* **2010**, *51*, 4231–4237. [CrossRef]

31. Leszczyńska, A.; Njuguna, J.; Pielichowski, K.; Banerjee, J.R. Polymer/montmorillonite nanocomposites with improved thermal properties. Part I. Factors influencing thermal stability and mechanisms of thermal stability improvement. *Thermochim. Acta* **2007**, *453*, 75–96. [CrossRef]

32. Liu, H.; Mead, J.L.; Stacer, R.G. Thermoplastic elastomers and rubber-toughened plastics from recycled rubber and plastics. *Rubber Chem. Technol.* **2002**, *75*, 49–63. [CrossRef]

33. Beaumont, N.J.; Aanesen, M.; Austen, M.C.; Börger, T.; Clark, J.R.; Cole, M.; Hooper, T.; Lindeque, P.K.; Pascoe, C.; Wyles, K.J. Global ecological, social and economic impacts of marine plastic. *Mar. Pollut. Bull.* **2019**, *142*, 189–195. [CrossRef] [PubMed]

34. Phelan, A.A.; Ross, H.; Setianto, N.A.; Fielding, K.; Pradipta, L. Ocean plastic crisis—Mental models of plastic pollution from remote Indonesian coastal communities. *PLoS ONE* **2020**, *15*, e0236149. [CrossRef] [PubMed]

35. Bidegain, G.; Paul-Pont, I. Commentary: Plastic waste associated with disease on coral reefs. *Front. Mar. Sci.* **2018**, *5*, 5. [CrossRef]
36. Ryan, P.G. Land or sea? What bottles tell us about the origins of beach litter in Kenya. *Waste Manag.* **2020**, *116*, 49–57. [CrossRef] [PubMed]
37. Lindsey, C.R.; Barlow, J.W.; Paul, D.R. Blends from reprocessed coextruded products. *J. Appl. Polym. Sci.* **1981**, *26*, 9–16. [CrossRef]
38. Bertin, S.; Robin, J.J. Study and characterization of virgin and recycled LDPE/PP blends. *Eur. Polym. J.* **2002**, *38*, 2255–2264. [CrossRef]
39. Larsen, Å.G.; Olafsen, K.; Alcock, B. Determining the PE fraction in recycled PP. *Polym. Test.* **2021**, *96*, 107058. [CrossRef]
40. Strapasson, R.; Amico, S.C.; Pereira, M.F.R.; Sydenstricker, T.H.D. Tensile and impact behavior of polypropylene/low density polyethylene blends. *Polym. Test.* **2005**, *24*, 468–473. [CrossRef]
41. Fonseca, C.A.; Harrison, I.R. An investigation of co-crystallization in LDPE/HDPE blends using DSC and TREF. *Thermochim. Acta* **1998**, *313*, 37–41. [CrossRef]
42. Zhao, L.; Choi, P. A review of the miscibility of polyethylene blends. *Mater. Manuf. Process.* **2006**, *21*, 135–142. [CrossRef]
43. Hossen Beg, M.D.; Bin Kormin, S.; Bijarimi, M.; Zaman, H.U. Effects of different starch types on the physico-mechanical and morphological properties of low density polyethylene composites. *J. Polym. Eng.* **2015**, *35*, 793–804. [CrossRef]
44. Tashiro, K.; Izuchi, M.; Kobayashi, M.; Stein, R.S. Cocrystallization and Phase Segregation of Polyethylene Blends between the D and H Species. 3. Blend Content Dependence of the Crystallization Behavior. *Macromolecules* **1994**, *27*, 1221–1227. [CrossRef]
45. Datta, N.K.; Birley, A.W. ThermaL Analysis of Polyethylene Blends. *Plast. Rubber Processing Appl.* **1982**, *2*, 237–245.
46. Lipatov, Y.S.; Moisya, Y.G.; Semenovich, G.M. Packing density of the chains in the boundary layers of polymers. *Polym. Sci. U.S.S.R.* **1977**, *19*, 146–151. [CrossRef]
47. Ström, G.; Fredriksson, M.; Stenius, P. Contact angles, work of adhesion, and interfacial tensions at a dissolving Hydrocarbon surface. *J. Colloid Interface Sci.* **1987**, *119*, 352–361. [CrossRef]
48. Krump, H.; Luyt, A.S.; Molefi, J.A. Changes in free surface energy as an indicator of polymer blend miscibility. *Mater. Lett.* **2005**, *59*, 517–519. [CrossRef]
49. Kratofil, L.J.; Ptiček, A.; Hrnjak-Murgić, Z.; Jelenčić, J.; Mlinac-Mišak, M. Compatibilization effects in SAN/EPDM blends prepared by reactive extrusion. *J. Elastomers Plast.* **2007**, *39*, 371–382. [CrossRef]
50. Ptiček Siročić, A.; Hrnjak-Murgić, Z.; Jelenčić, J. The surface energy as an indicator of miscibility of SAN/EDPM polymer blends. *J. Adhes. Sci. Technol.* **2013**, *27*, 2615–2628. [CrossRef]
51. Taheri, M.; Morshedian, J.; Khonakdar, H.A. Effect of compatibilizer on interfacial tension of SAN/EPDM blend as measured via relaxation spectrums calculated from Palierne and Choi-Schowalter models. *Polym. Bull.* **2011**, *66*, 363–376. [CrossRef]
52. Abhilash, S.S.; Luckose, R.; Lenin Singaravelu, D. Processing and characterization of HDPE and MDPE processed by rotational moulding. *Mater. Today Proc.* **2019**, *27*, 2029–2032. [CrossRef]
53. ExxonMobil Vistalon[TM] 404 Ethylene Propylene Copolymer Rubber Datasheet. Available online: http://www.lookpolymers.com/polymer_ExxonMobil-Vistalon-404-Ethylene-Propylene-Copolymer-Rubber.php (accessed on 2 March 2022).
54. OR.190222 (HDPE) Technical Data Sheet|Oceanworks. Available online: https://app.oceanworks.co/products/rec1efHk9KpfO9POU/tds (accessed on 28 February 2022).
55. OR.190252 (PP) Technical Data Sheet|Oceanworks. Available online: https://app.oceanworks.co/products/rec2Qj7VUBZackzFU/tds (accessed on 28 February 2022).
56. ExxonMobil ExxonMobil[TM] LDPE LD 123.LN Low Density Polyethylene Resin. Available online: https://exxonmobilchemical.ulprospector.com/en-US/ds243948/ExxonMobil%E2%84%A2%20LDPE%20LD%20123.LN.aspx?I=58933&U=0 (accessed on 25 February 2022).
57. Certene®SGM-140—Muehlstein—Datasheet. Available online: https://omnexus.specialchem.com/product/t-muehlstein-certene-sgm-140 (accessed on 25 February 2022).
58. ExxonMobil Paxon[TM] BA50-100 High Density Polyethylene Resin. Available online: https://exxonmobilchemical.ulprospector.com/en-US/ds244451/Paxon%E2%84%A2%20BA50-100.aspx?I=58933&U=1 (accessed on 25 February 2022).
59. Martey, S.; Addison, B.; Wilson, N.; Tan, B.; Yu, J.; Dorgan, J.R.; Sobkowicz, M.J. Hybrid Chemomechanical Plastics Recycling: Solvent-free, High-Speed Reactive Extrusion of Low-Density Polyethylene. *ChemSusChem* **2021**, *14*, 4280–4290. [CrossRef] [PubMed]